Fibers and Polymers (2023) 24:1771–1779
https://doi.org/10.1007/s12221-023-00044-8

Online ISSN 1875-0052
Print ISSN 1229-9197

REGULAR ARTICLE

Corn Stalk Biochar-Reinforced High-Density Polyethylene Material: Flame-Retardant and Anti-aging Properties

Yazhen Wang[1,2,3] · Xinyu Liu[1,2] · Tianyu Lan[1,2] · Qing Yang[1,2] · Shanshan Cong[1,2] · Yuxin Lin[1,2]

Received: 10 January 2022 / Revised: 18 May 2022 / Accepted: 12 June 2022 / Published online: 21 March 2023

Abstract

Corn stalk biochar (CSB), which was prepared from corn stalk (CS), was used to strengthen high-density polyethylene (HDPE). CSB/HDPE composite (CSBH) was prepared by extrusion. In this paper, we studied the effect of CSB on flame retardancy and aging resistance of HDPE. CSB and CSBH were characterized via scanning electron microscopy (SEM), thermogravimetric analysis (TGA), Fourier transform infrared spectroscopy (FTIR), X-ray photoelectron spectroscopy (XPS), limit oxygen index tester (LOI), and miniature combustion calorimeter (MCC). The results showed that, compared with CS, the aromatization degree of CSB increased. Compared with HDPE, the anti-aging properties of CSBH were significantly improved. SEM results showed that the surface of CSBH was still smooth after 28 days of aging treatment, and the carbonyl index (CI) did not change much. With the addition of CSB, the flame-retardant properties of HDPE material were enhanced. The TGA diagram confirmed that CSB improved the stability of HDPE material. In summary, biochar is able to enhance thermal stability, flame-retardant, and anti-aging properties of biocomposites.

Keywords HDPE · Biochar · Thermal stability · Anti-aging · Flame retardant

1 Introduction

Considering the massive waste of resources and serious environmental pollution, human beings must reconsider the current patterns of development and focus on environmental conservation [1, 2]. In recent years, biochar, serving as the soil conditioner and sustained-release carrier of fertilizer, has gained more attention. And a great progress has been made in the application of biochar for carbon sequestration [3]. Biochar is not only widely used in agriculture and forestry, but also developed rapidly in the formation of composite materials. As a new type of environmentally friendly material, biochar/plastic composite material is showing more potential for development [4]. As a renewable, microporous, and carbon-rich material, biochar is widely used in polymer reinforcement systems. It is a product of biomass pyrolysis with higher stability [5, 6]. Polyethylene (PE) is widely used in industries of printing, electrical appliances, cables, chemicals, and coal [7]. High-density polyethylene (HDPE) and low-density polyethylene (LDPE) are the two main types of PE. PE is a kind of flammable material, so it needs flame-retardant treatment. In addition, HDPE produces a large amount of droplets during its burning process, which is a fire hazard. As a result, it is very important to modify its flame retardancy [8]. Anti-aging performance is also crucial to polymers. Saturated polyolefin materials are often susceptible to oxidation and carry carbonyl groups, peroxide hydroxyl groups or double bonds during synthesis, thermal processing, long-term storage and use. Consequently, most polydiameter materials are not resistant to ultraviolet (UV) light. Therefore, it is necessary to study the anti-aging properties of HDPE. The aging mechanism of HDPE is shown in Fig. 1 [9]. In the UV aging process, there are two primary chain-breaking reactions, Norrish type I and type II, which produce carbonyl and vinyl groups. And

✉ Yazhen Wang
wyz6166@nefu.edu.cn

✉ Tianyu Lan
409222743@qq.com

1 College of Materials Science and Engineering, Qiqihar University, Qiqihar 161006, Heilongjiang, China

2 Heilongjiang Key Laboratory of Polymer Matrix Composites, Qiqihar 161006, China

3 College of Chemistry, Chemical Engineering and Resource Utilization, Northeast Forestry University, Harbin 150040, Heilongjiang, China

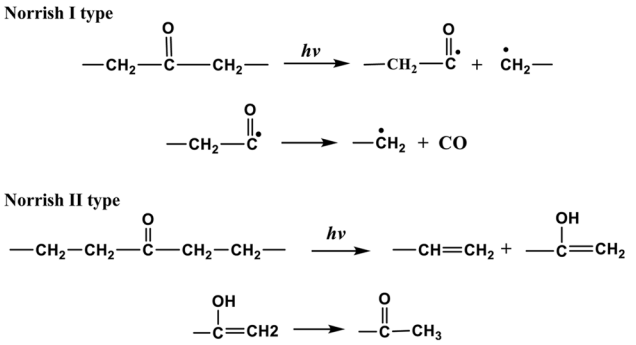

Fig. 1 HDPE aging degradation mechanism

the short chains after chain breaking will be crosslinked. Many scholars take the carbonyl group as the characteristic group of UV aging photochemical reaction.

So far, few research has been done on the effect of biochar-reinforced polymer materials on the anti-aging properties. In this paper, CSBH was prepared by extrusion. The flame-retardant and anti-aging properties of CSB-enhanced HDPE composites were systematically studied, which can broaden the applications of CSBH and provide a theoretical foundation for them.

2 Experiment

2.1 Materials

HDPE, melt flow rate 3.2 g/10 min, density 0.961 g/cm^3, Shanghai Tanxin Technology Co., LTD. CS, over 100 mesh, Gannan County, Qiqihar City, Heilongjiang Province; hydrochloric acid (HCl), analytically pure, Tianjin Fuyu Fine Chemical Co., LTD; maleic anhydride (MA), density 0.92 g/mL, Shandong Xinheng Chemical Co., LTD.

2.2 Preparation of CSB

The treated CS was cleaned for six times to remove the dust on the surface, and then dried for 24 h in an oven at 70–80 °C. The CS was wrapped in tinfoil, and placed in a crucible. And then it was put in a programmable Muffle furnace with a heating rate of 3 °C/min. After reaching 500 °C, it was kept for 2 h, and then cooled to room temperature. After that, it was treated with hydrochloric acid (1 mol/L) for 4 h. Then it was washed with distilled water until the pH of the liquid is 7. This carbonized product was dried at 70–80 °C for 24 h. And then the product was sifted with a 100-mesh sieve for later use.

2.3 Preparation of CSBH

CSBH was prepared by blending CSB with HDPE after adding MA. The mass of MA is equal to that of 3% CSB relatively. The materials were put in a high-speed mixer (GRH-10) to get the uniform blends before being extruded through a twin-screw extruder (SHJ-20B). The temperature of the nozzle is set to 185 °C. From the first zone to the fifth zone of the extruder, the temperatures were kept at 170, 175, 180 185, and 190 °C, respectively. Then the products from the extruder were dried for 12 h at 80 °C. Afterward, an injection molding machine (SSF380-K5) was used to get standard samples. The melt temperature was set at 185 °C and the injection pressure was 100 MPa.

For instance, the mixture was named as 20CSBH when the mass fractions of CSB and HDPE were 20 and 80 wt%, respectively. The mixtures contained CSB ranging from 20 to 60 wt% with an interval of 10 wt% each, and the samples under different CSB loadings were named as 20CSBH, 30CSBH, 40CSBH, 50CSBH, and 60CSBH, respectively. These samples were stored at room temperature for 24 h for testing.

3 Analysis

3.1 Fourier Transform Infrared Spectroscopy (FTIR)

The changes of functional groups on the surface of the dry material were measured by FTIR spectrometer (Spectrum One). The material was mixed with potassium bromide in a ratio of 1:2000. And it was ground in an agate mortar and pressed into tablet form for testing. Scanning was performed for 32 times in the scanning range of 4000–500 cm^{-1} and a spectral resolution of 4 cm^{-1}.

3.2 X-Ray Photoelectron Spectroscopy (XPS)

The changes of elements and structures of CS and CSB were analyzed via X-ray photoelectron spectrometer (ESCALAB250X). To determine changes of carbon bonds, peak differentiating and imitating of C element in the XPS spectrum had been conducted. The vacuum degree of the system was set as 7–9 mbar. The whole spectrum and C element were scanned.

3.3 Thermogravimetric Analysis (TGA)

TGA is a common method for determining selected characteristics of materials that show mass loss or gain caused by decomposition, oxidation, or loss of volatiles. TGA was

performed using a thermogravimetric analyzer (Q500) in nitrogen (20 ml/min). The scanning temperature ranged from 30 to 600 °C, and the heating rate was 10 °C/min. And the weight of each sample was approximately 10 mg.

3.4 Flame-Retardant Properties of HDPE and CSBH

3.4.1 Limiting Oxygen Index (LOI) Test

The test was conducted by a limit oxygen index tester (JF-3), and the size of the sample was $160 \times 10 \times 4$ mm^3. Each group of samples was tested for five times to take the average value. A line at a distance of 25 mm to one end of the sample was drawn, and another line was drawn at a distance of 125 mm to the same end of the sample. According to China's national standard GB/T2406.2-2009 (Plastics-Determination of Burning Behavior by Oxygen Index-Part 2: Ambient-Temperature Test), the test was conducted through the method of top ignition with the airflow rate of 10 L/min.

3.4.2 Miniature Combustion Calorimeter (MCC) Test

The heat release rate and total heat release of CSBH with different CSB contents were measured by a miniature calorimeter (FTT0001-11311).The test was conducted in a mixed air flow (flow rate of N_2: 80 ml/min; flow rate of O_2: 20 ml/min) with a heating rate of 1 °C/s and a temperature range of 150–700 °C.

3.5 Anti-aging Performance of Composite Materials

Ultraviolet aging tests were carried out on the HDPE and CSBH using artificial accelerated aging testing machine (QUV). The blackboard temperature of the machine was set at 70 °C and the ultraviolet radiation intensity was 0.89 W/m^2. The lengths of time for artificial accelerated aging tests were 0, 7, 14, 21, and 28 days, respectively. After each sample was taken out, the ultraviolet radiation intensity and temperature of the testing machine were corrected to ensure the accuracy of the experimental results. Manual accelerated aging test was conducted according to technical standard ASTMG53-88.

3.5.1 Surface Morphology Analysis Before and After Aging (SEM)

A scanning electron microscope (S-3400) was used to study the surface morphology of HDPE and CSBH before and after aging. The surfaces of the materials were sprayed with gold before testing.

3.5.2 Mechanical Properties

The flexural strength and tensile strength of HDPE and CSBH samples before and after aging were tested by universal testing machine (WSM-20KN, Changchun Intelligent Instrument Equipment Co., LTD.) according to China's national standards. Flexural samples (GB/T9341-20M8, China, $80 \times 10 \times 4$ mm^3) and tensile samples (GB/T13525-92, China, $160 \times 10 \times 4$ mm^3) were tested. Each sample was tested five times to take the average value.

3.5.3 Carbonyl Index

FTIR spectrometer (Spectrum One) was used to determine the changes of functional groups in HDPE and CSBH [10]. The carbonyl index (CI) was calculated by: C1 = A1/A2.where A1 and A2 are the integral areas of the carbonyl part and the invariant groups, respectively.

4 Results and Discussion

4.1 FTIR Analysis of CS and CSB

As shown in Fig. 2, the peak at 3408 cm^{-1} belonged to the stretching vibration of the unstable functional group O–H. The absorption peak intensity of O–H in the carbonized product decreased, which proved that the stability of the material after carbonization enhanced; the peak at 2916 cm^{-1} was contributed by the C–H stretching vibration of the alkyl chain. The spectrum of CSB did not have this peak here, indicating that after carbonization, the aliphatic alkyl chain was lost due to the tendency of the alkyl chain to aromatization; compared with the spectrum of CS, there

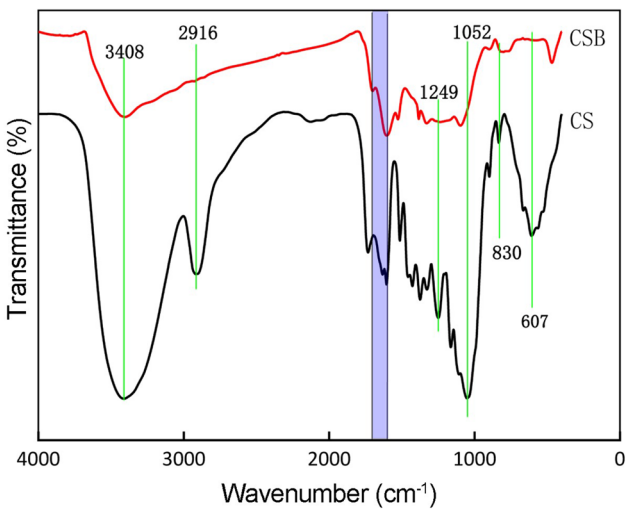

Fig. 2 Infrared spectra of CS and CSB

were no peaks belonging to flexural vibration of C–O–C at 1249 and 1052 cm^{-1} in the spectrum of CSB, indicating that high temperature caused biomass bonds to break and a large number of oxygen-containing functional groups decomposed; the two absorption peaks at 830 and 607 cm^{-1} belonged to the aromatic ring structure and Si–O, respectively [11]. The decrease in the peak value of Si–O might be related to post-processing; the blue area in the figure indicated that the material contained quinone-like and aromatic ketone groups. The above results indicate that the stability of the product after carbonization is enhanced.

4.2 XPS Analysis of CS and CSB

The structures of CS and CSB were identified by qualitative analysis and quantitative calculation using XPS. As shown in Fig. 3a, CS surface mainly contained C element, O element, and a small amount of Si element. Strong peaks at 284–290 eV and 532 eV belonged to C element and O element, respectively. Compared with CS, the carbon content of carbonized CSB was relatively increased, and the oxygen content is relatively reduced. As shown in Fig. 3b and c, the carbon spectra of each structure were obtained through the C1s peak separation processing of CS and CSB. Compared with other chemical bonds, the relative proportion of C–C bonds was the highest. The reason is that the content of cellulose and hemicellulose in the outer layer is lesser than that of lignin. The structures and properties of CS and CSB were mainly determined by the binding mode and state of C element. It is indicated in Fig. 3 that C–C and C–H were the main bonds in CS and CSB, meaning that the main structure of the outermost layer was long-chain aliphatic hydrocarbon.

After carbonization, the relative strength of each bond changed significantly. Compared with the CS in Fig. 3b, the relative proportion of C–O in CSB in Fig. 3c increased and the relative proportions of C–C and C = O decreased, showing that the degree of aromatization of CS after carbonization increased. The main reason is that high temperature will aggravate the condensation reaction, and C = O will be oxidized to C–O in varying degrees, which is consistent with the above-mentioned infrared analysis results.

4.3 TG Analysis of HDPE and CSBH

The TG and DTG curves of HDPE and CSBH are shown in Fig. 4. The mass loss curves and mass loss rate curves are shown in Fig. 4a and b, respectively. It can be seen from the figure that the degradation of HDPE started at about 450 °C and became stable after 500 °C. At about 480 °C, there was the most intense degradation. This result is the typical thermal decomposition process of HDPE [12]. As shown in Fig. 4, the amount of residue after thermal degradation of HDPE material was almost zero. Compared with pure

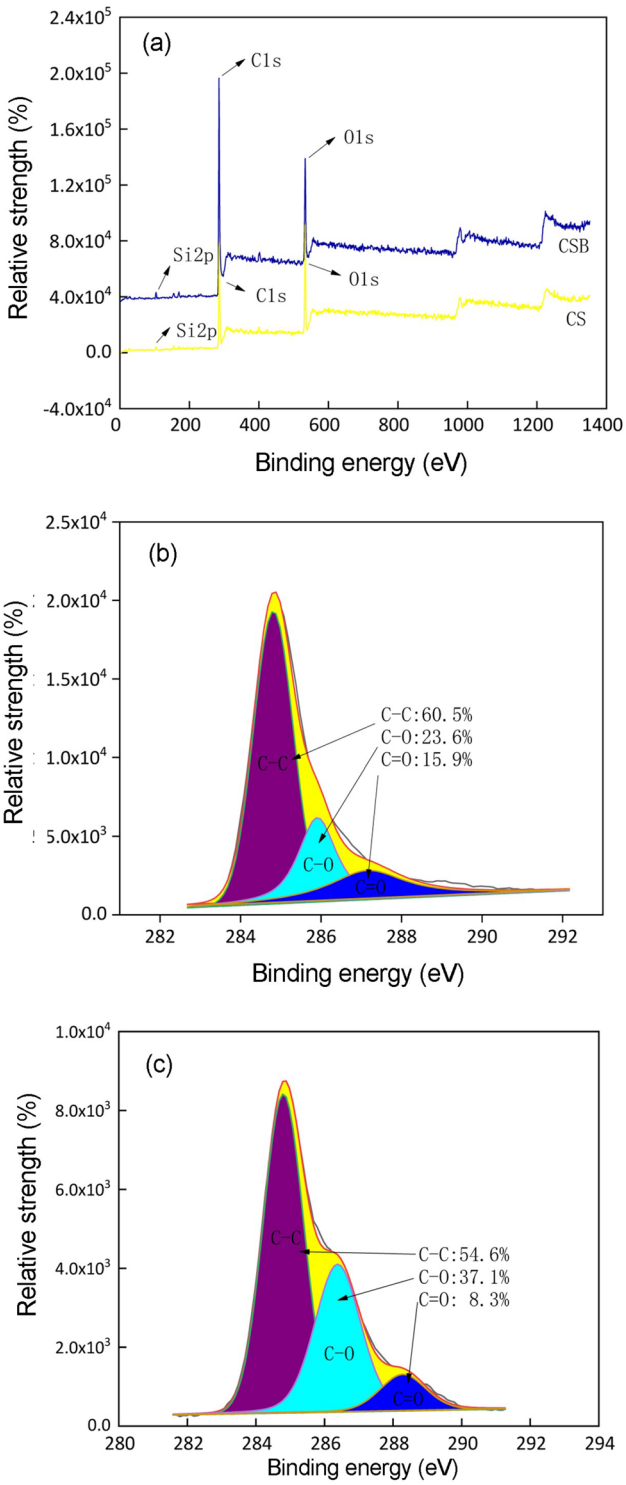

Fig. 3 XPS spectra of CS and CSB

HDPE, the more the CSB was added in HDPE, the more residue remained. The amount of residue was positively correlated with the content of CSB, proving that the addition of biochar enhanced the thermal stability of HDPE. This is because the enrichment of stable silica in biochar should be

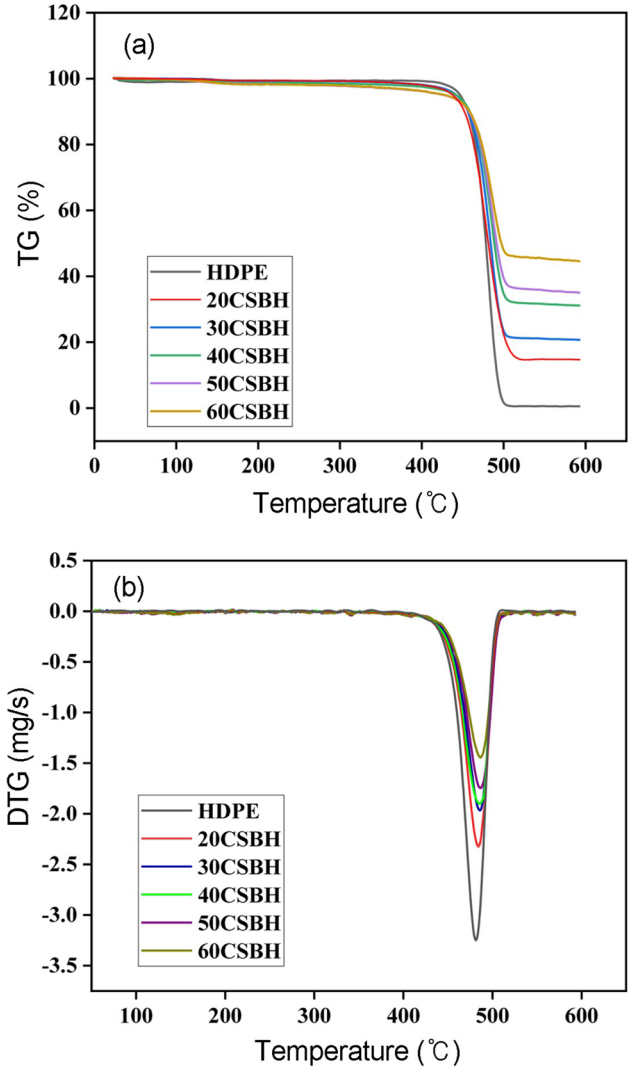

Fig. 4 TGA values of HDPE and CSBH

related to the amount of residue [13]. In summary, biochar shows great potential and benefits in preparing materials with high thermal stability.

4.4 Flame-Retardant Properties of HDPE and CSBH

4.4.1 Limiting Oxygen Index (LOI) Analysis

Since outdoor application of composite materials was determined by flammability, the LOI measurement was conducted to characterize the flame-retardant properties of HDPE and CSBH. As shown in Fig. 5, HDPE has the LOI of 18.6%, indicating poor flame retardancy [14]. It should be noted that the LOI of HDPE increased with CSB content, indicating that the addition of CSB in HDPE can improve its flame retardancy. As mentioned earlier, the addition of CSB improved the thermal stability of HDPE. Therefore, it can be

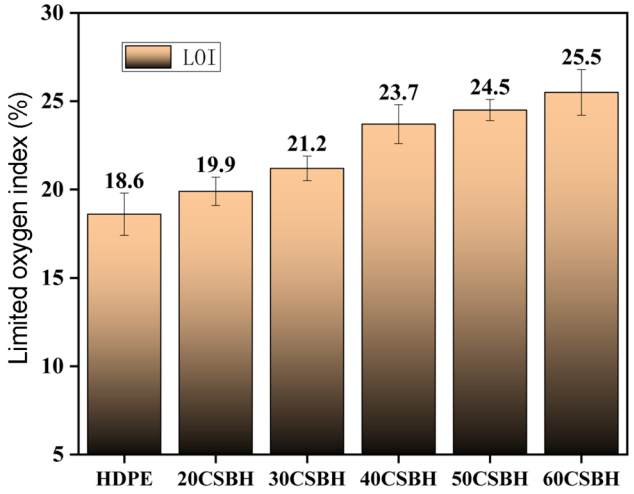

Fig. 5 LOI of HDPE and CSBH

said that the improvement of the flame retardancy of HDPE is obtained by adding CSB, which can be attributed to the fact that CSB with high thermal stability hinders the heat transfer between the heat source and HPDE [15]. In addition, it was reported that a large number of metal oxides and inorganic substances were produced in the preparation process of biochar accompanied by carbonization [16, 17]. These non-combustible metal oxides and inorganic substances, serving as flame retardants, can effectively slow down the combustion of HDPE and improve the flame retardancy of HDPE. The LOI reached a maximum of 25.5% when the CSB content was 60%, suggesting that adding biochar to HDPE can improve the flame retardancy. In summary, CSBH possesses potential in flame retardancy.

4.4.2 Miniature Combustion Calorimeter (MCC) Analysis

HRR refers to the heat release per unit mass of material combustion, and its peak value is PHRR. HRR curve can characterize the speed and size of heat release from material combustion. The MCC test data of HDPE and CSBH are shown in Table 1. As shown in Fig. 6, the HRR curve of pure HDPE is at the top and covers the largest area. With the

Table 1 HDPE and CSBH MCC test data

Samples	PHRR(w/g)	THR(KJ/g)	HRC(J/g k^{-1})
HDPE	1186.7	43.5	1583
20CSBH	1073.0	37.8	1106
30CSBH	914.1	33.0	936
40CSBH	753.0	29.3	770
50CSBH	684.1	27.6	702
60CSBH	639.6	24.1	664

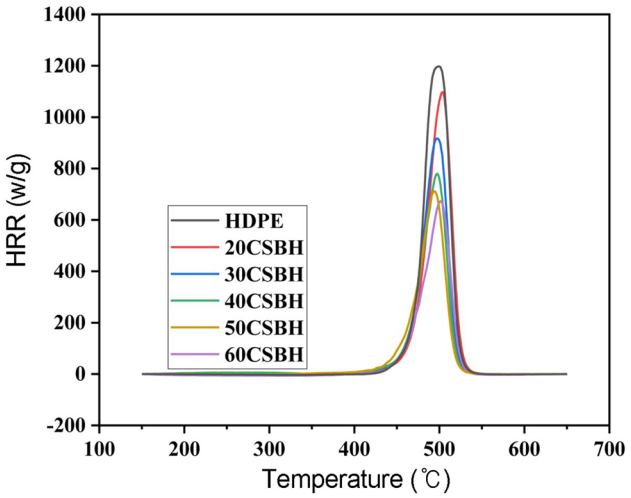

Fig. 6 MCC curve of HDPE and CSBH

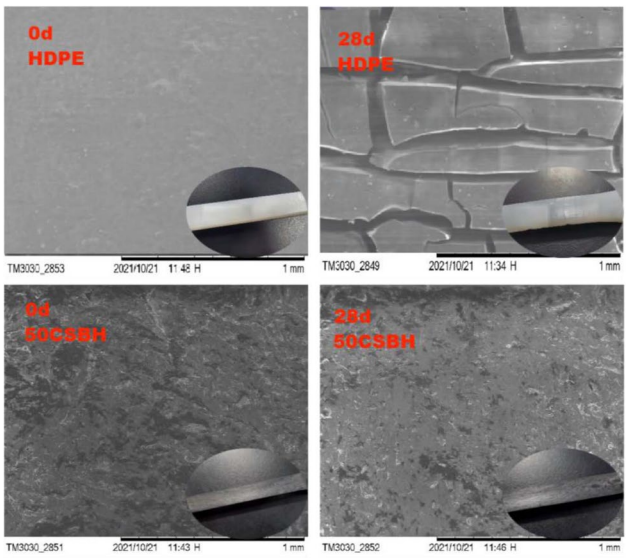

Fig. 7 Surface morphology of HDPE and 50CSBH before and after aging

increase of CSB content, the HRR curve of CSBH tended to be lower than that of pure HDPE, and the decrease amplitude increased with the increase of CSB content. PHRR of HRR curve also showed the same trend, and the PHRR of pure HDPE was 1186.7W/g. When the CSB content was 60%, the PHRR of 60CSBH was only 639.6 W/g, decreasing by 46.1%. THR refers to the total amount of heat released from combustion. The lower THR is, the less heat releases from material combustion, the better its flame retardancy is. In microcalorimetric test, THR also showed a similar trend to HRR. The THR of HDPE was 43.5 kJ/g, and the THR value decreased with the increase of CSB content. When the CSB content was 60%, the THR value of 60CSBH was only 24.1 kJ/g, which was 44.6% lower than that of pure HDPE. The heat released from CSBH combustion was significantly reduced. Heat release capacity (HRC), as a predictor of fire flammability, represents the maximum capacity of a material to release heat from combustion. The HRC value of pure HDPE was up to 1583 J/g k^{-1}, and tended to decrease with the increase of CSB content. The HRC value of 60CSBH was 664 J/g k^{-1}, which was 58.1% lower than that of HDPE. This can be attributed to the reduction of the maximum mass loss rate and combustion heat of decomposition products at this temperature [18]. The changes of comprehensive HRR curve, PHRR, and HRC were consistent with the TG analysis results. The addition of CSB can effectively reduce the combustion intensity and speed of HDPE, and effectively improve the flame retardancy of HDPE.

4.5 Anti-aging Properties of HDPE and CSBH

In the previous studies, the mechanical properties were the best when the CSB content was 50% [19]. Therefore, 50CSBH and HDPE materials were used for experiments in this paper to explore the changes of materials before and after aging.

4.5.1 HDPE and 50CSBH Surface Morphology Analysis (SEM) Before and After Aging

As shown in Fig. 7, before aging, the surface of HDPE material could be seen to be smooth via SEM even at a magnification of 100. Compared with the unaged material, obvious cracks appeared on the surface of the material after aging. The occurrence of cracks would inevitably cause decline in the mechanical strength of material. The main reason for this phenomenon may be the photochemical degradation reaction of polyethylene under the irradiation of ultraviolet light, making longer molecular chains break and form short molecular chains. The strength of the polyethylene material decreased with the decrease of molecular weight. Under the action of cohesion, the aging polyethylene material was broken, and the cracks appeared.

Compared with the 50CSBH before aging, no cracks were found in the 50CSBH after aging, showing obvious anti-aging phenomenon. The mechanical performance was reduced. The reason may be the good interface interaction between the rough structure of the CSB surface and the HDPE matrix, which can hinder cracks on the material.

4.5.2 Tensile and Flexural Strength of HDPE and 50CSBH Before and After Aging

Figure 8 shows the tensile and flexural strengths of HDPE and 50CSBH before and after aging. It can be seen that the mechanical and tensile properties of HDPE materials

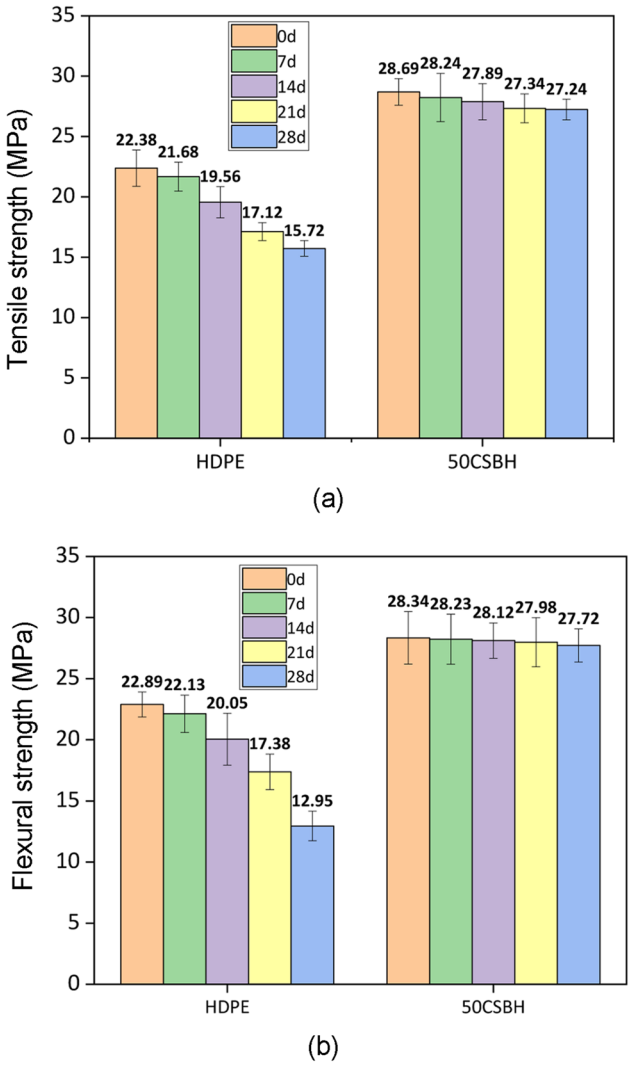

Fig. 8 Tensile and flexural strength of HDPE and 50CSBH before and after aging

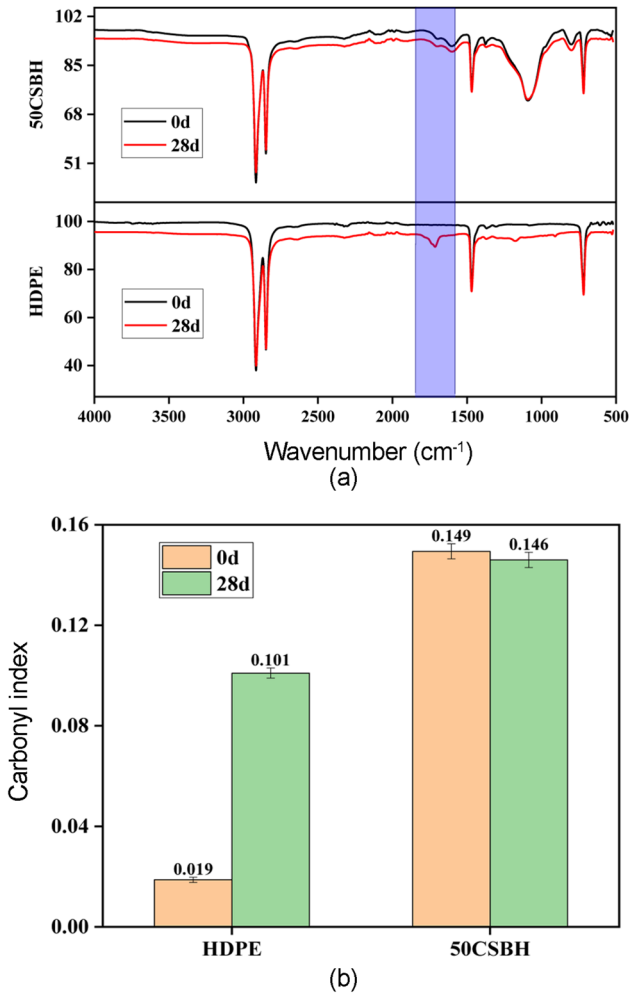

Fig. 9 Carbonyl changes of HDPE and 50CSBH before and after aging

decreased significantly with the increase in length of aging time. After 28 days of aging, the tensile strength and flexural strength of HDPE decreased by 29.76 and 43.43%, respectively. Compared with HDPE, the mechanical properties of 50CSBH changed a little before and after aging. In accordance with the above-mentioned SEM analysis, no cracks occurred on the surface of 50CSBH after aging, while cracks were obvious on the surface of HDPE material after aging. It was worth noting that the mechanical properties of HDPE decrease significantly with the increase in length of aging time. This is because HDPE material degraded under ultraviolet light, and chains were broken according to Norrish type I or II degradation mechanism, which made the number of carbonyl groups gradually increase and then showed serious aging phenomenon.

4.5.3 Mechanism of CSB Enhancing Anti-aging of HDPE Material

Figure 9a demonstrates the infrared spectrum of HDPE and 50CSBH before and after aging. The blue part is the position of C = O. After the aging of HDPE, the stretching vibration peak of C = O near 1700–1750 cm^{-1} was significantly enhanced, indicating that oxidation occurred on the surface of HDPE after UV irradiation. The peak value of 50CSBH changed only a little before and after aging. Carbonyl index (CI) was used as the evaluation standard of material aging degree. The faster the growth of the carbonyl index, the faster the degradation reaction [20]. Changes of CI are shown in Fig. 9b. After 28 days of aging, the CI of HDPE material showed an upward trend, indicating that it degraded under UV light and chains were broken according to Norrish type I or II degradation mechanism, which made the number of carbonyl groups gradually increase. It can be seen from the comparison of CI that after adding CSB to

the HDPE materials, 50CSBH had a significant increase in CI before aging. This is because carbonyl functional groups exist in the lignin component of CSB. As a result, adding CSB to HDPE is equivalent to introducing more carbonyl functional groups. Compared with 50CSBH before aging, the carbonyl index of it decreased slightly after aging. This is mainly due to the similar anti-aging mechanism between CSB and carbon black. As shown in Fig. 2, the material contains aromatic ketones and quinone groups, which can quench excited state and capture free radicals of polymers. And the color of the material is pure black, which can absorb or shield a part of ultraviolet rays, reduce the absorption of ultraviolet rays by the composite material and slow the degradation of the composite material. With the increase in length of aging time, the surface of 50CSBH gradually dried, making CSB on the surface fell away. This may be the main reason for the slight decrease of carbonyl index.

In addition, lignin is contained in CSB. The hindered phenolic structure in lignin has an anti-aging effect, mainly because of the ability of the hindered phenolic structure to react with the free radicals generated by HDPE excitation. Figure 10 demonstrates the equation of the reaction mechanism. The mechanism of the reaction between the lignin in CSB and the free radicals generated by HDPE can be divided into three main steps:

The first step is the formation of phenoxy radicals, which was caused by the transfer of alkyl radicals generated by the excitation of HDPE alkyl chains to the polyphenol structure in lignin during UV-accelerated aging process; the second step is the generation of quinone radicals, which was triggered by the transfer of the instable phenoxy radicals to lower energy radicals; the last step is the inhibition of free radicals, which was caused by the chain-inhibition reaction between the generated quinone radicals and alkyl radicals excited by external factors, generating cyclohexadienyl peroxides. Anti-aging effect of CSBH was achieved due to the termination of free-radical chain reaction.

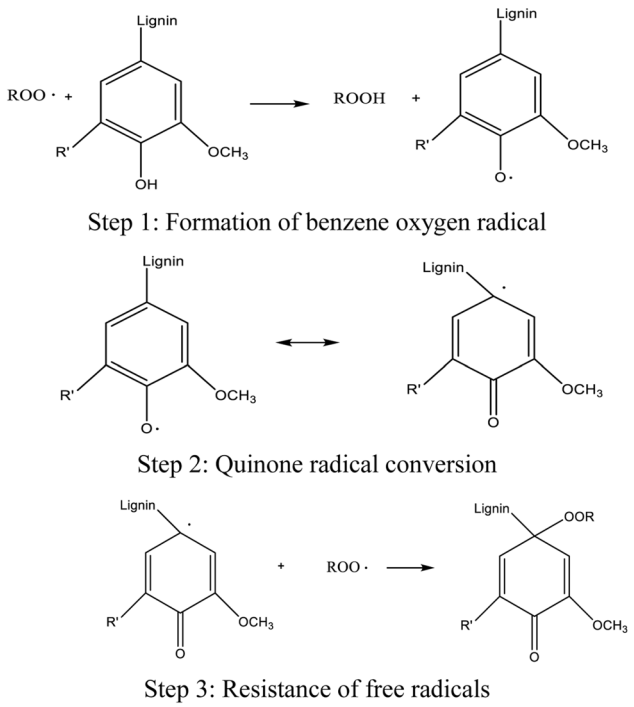

Fig. 10 Diagram of thermal aging resistance mechanism of lignin in CSB

Furthermore, lignin is also a UV shielding agent, because it has structures that can absorb UV light, including a large number of conjugated color-emitting groups like C = C, C = O, benzene rings, and quinone structure. These structures can create a barrier between CSBH and light radiation to absorb UV light, which can protect the interior of HDPE material from direct UV light and then inhibit the light aging of HDPE. However, it is worth noting that the anti-aging effect of lignin in CSB on HDPE is mainly dominated by the physical effect of light shielding and supplemented by the effect of hindered phenols and free radicals, because the hindered phenol structure is less active and less likely to react under light. These above-mentioned reasons may be responsible for the superior anti-aging properties of 50CSBH.

5 Conclusion

In this paper, we explored the flame-retardant and anti-aging properties of CSB-reinforced HDPE materials. The ultraviolet aging research was carried out by artificial accelerated ultraviolet aging treatment. And the anti-aging performance of HDPE and CSBH under different aging time was studied; the flame-retardant properties of HDPE and CSBH were studied by oxygen index tester and micro combustion calorimeter.

(1) XPS and FTIR spectra showed that compared with CS, the unstable oxygen-containing functional groups and aliphatic C–H bonds of carbonized CSB decreased or even disappeared. In addition, both the degree of aromatization and the stability of the material improved.
(2) TG and DTG showed that compared with pure HDPE, the more CSB was added into HDPE, the more material residue remained. And the amount of residue was positively correlated with the content of CSB, proving that the addition of biochar enhanced the thermal stability of HDPE.
(3) MCC and LOI showed that the addition of CSB increased the flame-retardant performance of HDPE material, and the flame-retardant properties were obviously enhanced with the increase of CSB content. Compared with HDPE, PHRR value of 60CSBH was

only 639.6 W/g, which indicates a decrease of 46.1%; the THR value of 60CSBH was only 24.1 kJ/g, which was 44.6% lower than that of pure HDPE; the HRC value of 60CSBH was 664 J/g k^{-1}, which was 58.1% lower than that of HDPE. It shows that the addition of CSB enhanced the flame-retardant properties of HDPE material.

(4) The addition of CSB improved the anti-aging properties of HDPE material. SEM showed that there was no crack on the surface of the 50CSBH before and after aging, and the carbonyl index does not change significantly compared with HDPE. To sum up, this paper broadens the application field of biochar polymer composites and improves the research value of bio-based composites.

Acknowledgements This work was supported by open project of Polymer matrix Composites Key Laboratory of Heilongjiang Province (No: 130712121025).

Data Availability The data that support the findings of this study are available from the corresponding author upon reasonable request.

Declarations

Conflict of Interest Authors have no conflict of interest to declare.

References

1. K. Beydoun, J. Klankermayer, Efficient plastic waste recycling to value-added products by integrated biomass processing[J]. Chemsuschem **13**(3), 488–492 (2020)
2. M.J. Ahmed, B.H. Hameed, Insight into the co-pyrolysis of different blended feedstocks to biochar for the adsorption of organic and inorganic pollutants: a review[J]. J. Clean. Prod. **265**, 121762 (2020)
3. Q.F. Zhang, W.M. Yi, Z.H. Li, L.H. Wang, H.Z. Cai, Mechanical properties of rice husk biochar reinforced high density polyethylene composites[J]. Polymers **10**(3), 286 (2018)
4. A. Khan, P. Savi, S. Quaranta, M. Rovere, M. Giorcelli, A. Tagliaferro, C. Rosso, C. Jia, Low-cost carbon fillers to improve mechanical properties and conductivity of epoxy composites[J]. Polymers **9**, 642 (2017)
5. D.B. Devallance, G.S. Oporto, P. Quigley, Investigation of hardwood biochar as a replacement for wood flour in wood-polypropylene composites[J]. J. Elastomers. Plast **48**(6), 510–522 (2016)
6. N. Nan, D.B. Devallance, X. Xie, J. Wang, The effect of biocarbon addition on the electrical, mechanical, and thermal properties of polyvinyl alcohol/biochar composites[J]. J. Compos. Mater. **50**(9), 1161–1168 (2016)
7. Q.F. Zhang, D.H. Zhang, H. Xu, W.Y. Lu, X.J. Ren, H.Z. Cai, H.W. Lei, E.G. Huo, F. Zhao, Q. Moriko, X.N. Lin, M.V. Elmar, M. Wendy, Biochar filled high-density polyethylene composites with excellent properties: towards maximizing the utilization of agricultural wastes[J]. Ind Crops Prod **146**, 112185 (2020)
8. Y.F. Shih, L.T. Wan, V.K. Kotharangannagari, Development of eco-friendly flame-retarded high density polyethylene composites[J]. Key Eng. Mater **847**, 55–60 (2020)
9. Z. Jia, J. Huang, Y. Gong, P. Jin, X. Suo, H. Li, Incorporation of copper enhances the anti-ageing property of flame-sprayed high-density polyethylene coatings[J]. J. Therm. Spray. Techn. **26**(3), 409–416 (2017)
10. M. Michalak, M. Hakkarainen, A.C. Albertsson, Recycling oxidized model polyethylene powder as a degradation enhancing filler for polyethylene/polycaprolactone blends[J]. ACS Sustain. Chem. Eng **4**, 129–135 (2016)
11. D.S. Bajwa, S.G. Bajwa, G.A. Holt, Impact of biofibers and coupling agents on the weathering characteristics of composites[J]. Polym. Degrad. Stab **120**, 212–219 (2015)
12. X. Lin, L. Kong, H. Cai, Q. Zhang, D. Bi, W. Yi, Effects of alkali and alkaline earth metals on the co-pyrolysis of cellulose and high density polyethylene using TGA and Py-GC/MS[J]. Fuel Process. Technol **191**, 71–78 (2019)
13. D.G. Bhowmick, A.K. Sarmah, R. Sen, Production and characterization of a value added biochar mix using seaweed, rice husk and pine sawdust: a parametric study[J]. J. Clean. Prod. **200**, 641–656 (2018)
14. D. Jiang, M. Pan, X. Cai, Y. Zhao, Flame retardancy of rice straw polyethylene composites affected by in situ polymerization of ammonium polyphosphate/silica[J]. Compos. Part A Appl. Sci. Manuf **109**, 1–9 (2018)
15. O. Das, D. Bhattacharyya, D. Hui, K.T. Lau, Mechanical and flammability characterisations of biochar/polypropylene biocomposites[J]. Compos. Part B Eng **106**, 120–128 (2016)
16. C. Chen, X. Yan, Y. Xu, B.A. Yoza, X. Wang, Y. Kou, H. Ye, Q. Wang, Q. Li, Activated petroleum waste sludge biochar for efficient catalytic ozonation of refinery wastewater[J]. Sci. Total Environ **651**, 2631–2640 (2019)
17. D. Wei, B. Li, H. Huang, L. Luo, J. Zhang, Y. Yang, J. Guo, L. Tang, G. Zeng, Y. Zhou, Biochar-based functional materials in the purification of agricultural wastewater: fabrication, application and future research needs[J]. Chemosphere **197**, 165–180 (2018)
18. K. Dai, S. Sun, W. Xu, B. Song, Y.Z. Deng, X.D. Qian, Covalently-functionalized graphene oxide via introduction of bifunctional phosphorus-containing molecules as an effective flame retardant for polystyrene[J]. RSC Adv **8**(44), 24993–25000 (2018)
19. Y.Z. Wang, X.Y. Liu, Z. Shi, Y.X. Lin, Y.H. Yang, S.B. Dong, T.Y. Lan, Rheological behavior of high density polyethylene (HDPE) filled with corn stalk biochar[J]. ChemistrySelect (2021). https://doi.org/10.1002/SLCT.202102663
20. N.M. Stark, L.M. Matuana, Surface chemistry changes of weathered HDPE/wood flow composites studied by XPS and FTIR spectroscopy[J]. Polym Degrad Stabil **86**, 19 (2004)